

Fingerprint Verification System Based on DWT, Multiple Domain Feature Extraction, and Ensemble Subspace Classifier

Sistema de verificación de huellas dactilares basado en DWT, extracción de características de múltiples dominios y clasificador subespacial de conjuntos

Sistema de verificação de impressão digital baseado em DWT, extração de recursos de vários domínios e classificador de subespaço de conjunto

Andres Rojas ¹, Gordana Jovanovic Dolecek ²

Recibido: Marzo 2022

Aceptado: Julio 2022

Summary. - This paper describes a fingerprint verification system including preprocessing, Wavelet transform, feature extraction using multiple domains, and ensemble subspace discriminant classifier. The system is implemented in MATLAB using Wavelet Toolbox, Image Processing Toolbox, and Statistics and Machine Learning Toolbox. First, the motivation and novelty, followed by the review of the previous work, are presented. Next, all steps are described in detail. Three fingerprint databases from the literature are used. The proposed method's performance is compared with state-of-the-art techniques based on different classifiers utilizing the accuracy metric. The proposed algorithm achieves high accuracy at 97.5% for the DB3-FVC2000 subset.

Keywords: fingerprint verification, image processing, classification learner, feature extraction, accuracy, ensemble subspace classifier.

Resumen. - Este documento describe un sistema de verificación de huellas dactilares que incluye preprocesamiento, transformada Wavelet, extracción de características utilizando múltiples dominios y clasificador discriminante subespacial de conjunto. El sistema se implementa en MATLAB utilizando Wavelet Toolbox, Image Processing Toolbox y Statistics and Machine Learning Toolbox. En primer lugar, se presenta la motivación y la novedad, seguido de la revisión del trabajo anterior. A continuación, se describen todos los pasos en detalle. Se utilizan tres bases de datos de huellas dactilares de la literatura. El rendimiento del método propuesto se compara con técnicas de última generación basadas en diferentes clasificadores que utilizan la métrica de precisión. El algoritmo propuesto logra una alta precisión del 97,5 % para el subconjunto DB3-FVC2000.

Palabras clave: verificación de huellas dactilares, procesamiento de imágenes, aprendizaje de clasificación, extracción de características, precisión, clasificador subespacial de conjunto.

¹ Bachelor of Science, Department of Electronics, National Institute of Astrophysics, Optics, and Electronics (INAOE), andres.rojas@inaoep.mx, ORCID iD: <https://orcid.org/0000-0003-1773-8514>

² Engineering Professor, Department of Electronics, National Institute of Astrophysics, Optics, and Electronics (INAOE), gordana@ieec.org, ORCID iD: <https://orcid.org/0000-0003-1258-5176>

Resumo. - Este documento descreve um sistema de verificação de impressão digital que inclui pré-processamento, transformada Wavelet, extração de recursos usando vários domínios e classificador discriminante de subespaço de conjunto. O sistema é implementado em MATLAB usando Wavelet Toolbox, Image Processing Toolbox e Statistics and Machine Learning Toolbox. A motivação e a novidade são apresentadas primeiro, seguidas pela revisão do trabalho anterior. Todas as etapas são descritas em detalhes a seguir. Três bancos de dados de impressões digitais da literatura são usados. O desempenho do método proposto é comparado com técnicas do estado da arte baseadas em diferentes classificadores que utilizam a métrica de precisão. O algoritmo proposto atinge uma alta precisão de 97,5% para o subconjunto DB3-FVC2000.

Palavras-chave: verificação de impressão digital, processamento de imagem, aprendizado de classificação, extração de recursos, precisão, classificador de subespaço de conjunto.

1. Introduction. - The fingerprint is one biometrics that fulfills two essential attributes for unambiguous recognition: uniqueness and stability over time. Fingerprints remain relatively unchanged for life, and even the fingerprints of identical twins are different [1]. The other two biometrics that fulfill these requirements are the face and iris [2]. Fingerprints are famous for many reasons, they are accessible, do not provide more information than necessary, such as an individual's race or health, and fingerprint sensors have a relatively low price [3].

There are many reasons to use biometrics, including improving the convenience and efficiency of routine access transactions, reducing fraud, and improving public safety and national security [4]. Nowadays, multiple devices have finger-imaging sensors that better protect them from intruders, another security measure in addition to the specific password, or even face recognition.

Commonly, low-cost sensors' fingerprints are low resolution; moreover, the scanner and acquisition software is not flexible to be customized. As a result, developers deal with low-resolution fingerprints in their applications. Since most early research relies on features such as ridges, delta, and core (minutiae) points, the location of these points needs to be determined. Although this process can be relatively simple for a human, it requires complicated computation to be extracted by a computer. This problem is even more complex for low-resolution fingerprint images since some ridges can be broken in the image and wrongly considered as the core [5].

Nowadays, researchers explore non-minutiae representations by considering fingerprint images as oriented textures that combine the global and local information in a fingerprint [1]. In this work, the focus is on non-minutiae techniques, which implies that there is no need to analyze every local feature in the fingerprint, but rather texture-based features are calculated. A complete image of a fingerprint cannot be used or processed every time because the memory required to perform that task can be enormous. This problem slows down the processing speed of the system for recognition. For this reason, only prominent features are extracted from each image, and a feature set is created [1]. Our hypothesis for this research states that implementing more texture descriptors leads to more accurate fingerprint verification results.

One of the most popular non-minutiae approaches is the Wavelet transform. This technique produces spatial, and frequency representations used to create features that describe the textural characteristics of a fingerprint. A fingerprint image has distinct features with some frequency and direction. The corresponding subimages have larger energies using the Wavelet transform. By applying the Wavelet transform, vital information of the original image is transformed into a compressed image without much loss of information. The Wavelet transform has been widely used in signal processing, pattern recognition, and texture recognition [6].

This compressed information can be obtained from the same subject with similar results creating a set that can be used for pattern classification. A supervised machine learning algorithm is helpful for fingerprint verification since it generates a model that learns from image data in the form of feature vectors. In the training stage, a model is generated from the input feature vectors and their expected output values (labels) to map any new data to one of the trained categories. The training data consist of a set of training examples, each group having a pair consisting of an input object and the desired output value. A supervised learning algorithm learns from this training pair relationship and produces an inferred function [7].

In ensemble classification, multiple homogeneous or heterogeneous classifiers are combined to solve a similar classification problem. This approach enhances the generalization of models and improves the classification results even using weak classifiers [8].

This paper presents an extended version of the fingerprint verification system based on the Wavelet transform and ensemble subspace discriminant classifier [9]. It contains a detailed description of the image processing techniques applied to the preprocessing algorithm and more information regarding the features computed to classify the fingerprint images. This extended version includes more classification results obtained from the 12 fingerprint image subsets analyzed in this work.

This paper is organized as follows: Section 2 elaborates on motivation and novelty, while the next

section presents a review of previous works on fingerprint recognition. A detailed description of the proposed method is presented in Section 4. Section 5 reports the main results and discussion, and Section 6 states the conclusions.

2. Motivation and novelty. - Fingerprints are images obtained when the fingertip surface touches another surface, and even on the same hand, each fingertip surface describes a different pattern. Each person has unique designs on each fingertip surface. The probability of coinciding with other fingerprints is almost zero [10]. Human fingerprints are mainly different, and the overall shape does not change over time which is beneficial for machine learning applications because a good classifier should be stable over time. Its inputs should be consistent inside their pattern realm. Below we present the principal motivations for the study of fingerprints:

- Fingerprint image databases highly depend on the finger's surface status including external variables such as humidity, dust, temperature, etc. These parameters affect the accuracy of the recognition system and make the identification process more difficult, especially with low-quality fingerprint datasets [10].
- A fingerprint recognition system requires a minimum Equal Error Rate (EER), possibly zero, to provide high accuracy values, which is one of the most critical parameters of a fingerprint recognition system [1].
- A complete fingerprint image cannot be used or processed every time as the memory required might be significant, which reduces the processing speed. Also, pixel-by-pixel comparison with the query image may consume most of the time of the processor and a shift by a one-pixel value may lead to a complete mismatch and pseudo results. Hence, only prominent features must be extracted from each image, and a feature database is formed [1].
- Ensemble classifiers have increasingly gained more attention in different pattern recognition applications. This classification method combines the results of classifiers with varying accuracy scores with different techniques (voting, average, etc.). Thus, it is possible to obtain better predictive results from a single classifier [11].
- Wavelets are used to decompose the fingerprint image into different levels of resolution to ease information interpretation. Wavelet coefficients are independent, creating a set of features of the actual fingerprint image at different resolutions, which is useful for classification purposes [6].

The above analysis shows the principal task in fingerprint processing. Our main objective and motivation for this research are to get high accuracy in verification; using ensemble classifiers may be very useful in this task. A comparison was performed with previous simple models to choose the correct classifier. The results show that the ensemble subspace provides the highest accuracy compared to other machine learning algorithms. Consequently, our approach is based on the ensemble subspace discriminant approach.

The implementation of ensemble subspace discriminant classifiers is reported in [12] related to liver fibrosis in mice microscopic images. This work computed morphological and statistical features such as the area, perimeter, circularity, mean, median, and mode from microscopic images. Another ensemble approach for classifying satellite images is reported in [13]. More recently, the project in [14] for biometric human footprint matching applied ensemble subspace discriminant classifiers combined with fuzzy logic. Finally, the work presented at URUCON 2021 reported in [9] is one of the newest fingerprint recognition systems based on an ensemble of Linear Discriminant Analysis (LDA) classifiers using the random subspace method. This system utilizes

preprocessing to enhance the fingerprint images in conjunction with multiple domain feature extraction techniques.

The novelty of this work is the application of multiple transforms for feature extraction of fingerprint images [9] to implement a fingerprint verification system simulated in MATLAB. This paper highlights essential details such as the preprocessing algorithm steps, multiple image processing techniques, and more insight into the feature extraction, especially texture descriptors.

3. Review of previous works. - The literature on fingerprint identification systems presents similar subsystems: input data processing, feature extraction, and classification [10]. The main differences between the existing systems generally consist of the feature extraction technique and the classification approach [10]. Since the method proposed here is based on the Wavelet transform, we will review some Wavelet transform-based strategies enhanced with different machine learning classifiers.

The authors in [15] proposed two methods to detect fingerprint images based on one-dimensional (1-D) and two-dimensional (2-D) Discrete Wavelet Transform (DWT). Three statistical parameters are used to evaluate those two methods: skewness, kurtosis, and convolution of the approximation coefficients of 1-D DWTs. The cross-correlation coefficient was used to classify the fingerprints of different persons.

Reference [16] presented Wavelet features extracted directly from gray-scale fingerprint images without preprocessing. This system was tested on a small fingerprint database using the k-NN classifier.

Wavelet co-occurrence features are reported in [17], these values are extracted from the approximation coefficients of fingerprint images and classified using a feedforward neural network. The four recognition Wavelet co-occurrence features are contrast, correlation, energy, and homogeneity.

The authors in [18] presented an approach based on combining multiple domains: spatial, Fourier, Discrete Cosine Transform (DCT), and Wavelet. This system was designed for matching poor-quality fingerprints using the Manhattan distance measure for classification. A Wavelet-Bands Selection Features (WBSF) technique is proposed in [19]. In this case, the Euclidean and City-Block distance measures performed the pattern matching process. The method reported in [6] uses robust local features extracted from Haar Wavelet subheads. The classification approach in this paper was based on the absolute difference between the feature vectors. Another Euclidean distance approach is reported in [20], where the feature extraction is based on blocks of an enhanced region of interest (ROI). The feature vectors consist of mean energy, standard deviation, and Shannon entropy. The authors in [5] applied a simple method to verify low-resolution fingerprints using Haar-like transformations to generate feature vectors. These vectors were verified against their reference counterparts using the Hamming distance.

It is common for many authors to apply a combination or a comparison of machine learning algorithms; for example, the authors in [21] proposed SVM and k-NN as classification methods. This work utilized three discrete feature extraction methods: DWT, Principal Component Analysis (PCA), and DCT. The fingerprint identification system in [22] was based on Gabor Wavelet and SVM, indicating that Gabor Wavelet features represent textural information at different scales and orientations, accomplishing high recognition rates using a well-tuned SVM. The authors in [7] implemented fingerprint classification using SVM and logistic regression classifiers. Ridge fingerprint contours were extracted using a canny edge detection filter, creating feature vectors. The fingerprint images were enhanced using Gabor filters and the Wavelet transform. A similar approach in [10] proposed developing a fingerprint identification system based on image processing methods that clarify fingerprint contours. The matching process applied one and two-layer perceptron neural networks, random forest, and SVM.

4. Description of the method. - In this work, the FVC2000 [23], FVC2002 [24], and FVC2004 [25] fingerprint databases were used. A database is composed of four subsets, and each subset has 80 fingerprint images acquired from 10 subjects with eight imprints. A total of 960 fingerprint images were applied for fingerprint recognition. Each subset presents distinct characteristics, including resolution, size, and quality. The steps of the proposed method are presented below.

Step 1: Preprocessing

A gray-level fingerprint image I is defined as a $M \times N$ matrix, where $I(i, j)$ represents the intensity of the current pixel located in the i th row and j th column. An orientation image O is defined as a $M \times N$ image, where $O(i, j)$ represents the local ridge orientation at pixel (i, j) . The local ridge orientation is generally specified for a block of pixels rather than one. Former implies that the fingerprint image is divided into $w \times w$ non-overlapping blocks, and a single local ridge orientation is defined for each block. When analyzing a fingerprint, we can notice that the local ridge orientations of 90° and 270° are the same since the ridges oriented at these angles in a local neighborhood cannot be differentiated. A frequency image F is a $M \times N$ image, where $F(i, j)$ represents the local ridge frequency defined as the frequency of the ridge-valley structure in a local neighborhood along the normal direction to the local ridge orientation. This image is specified in blocks as the orientation image. A region mask R is a $M \times N$ image, where $R(i, j)$ indicates the category of a pixel [26]. There are two possible categories:

- Recoverable pixel: Where a small amount of noise corrupts ridges and valleys, this could be in the form of scars, creases, smudges, etc. However, neighboring regions or pixels can provide information about the actual ridge-valley structures. These pixels are labeled with a value of 1.
- Unrecoverable pixel: Where ridges and valleys are corrupted with a significant amount of noise and distortion, making the structures not visible. The neighboring regions cannot provide information to recover the authentic ridge-valley shapes. These pixels are labeled with a value of 0.

Preprocessing of the input fingerprint images is needed before applying the Wavelet transform. This process involves image processing techniques such as normalization of intensities in the image, local orientation and frequency estimation, region mask estimation, Gabor filtering, and binarization to enhance the image [26, 27].

Normalization: This is a pixel-wise operation, and its objective is to clarify ridge-valley structures by reducing variations in gray-level values throughout the image. Let $I(i, j)$ denote the gray-level value of the pixel (i, j) , M , and VAR the mean and variance of I , respectively. $N(i, j)$ denote the normalized gray-value in the pixel (i, j) defined as:

$$N(i, j) = \begin{cases} M_0 + \sqrt{\frac{VAR_0(I(i, j) - M)^2}{VAR}}, & \text{if } I(i, j) > M \\ M_0 - \sqrt{\frac{VAR_0(I(i, j) - M)^2}{VAR}}, & \text{otherwise} \end{cases}, \quad (1)$$

where M_0 and VAR_0 are the desired mean and variance, respectively [26].

Local orientation estimation: An orientation image provides information about a fingerprint in oriented texture, an intrinsic property defined by invariant coordinates of ridges and valleys in a local neighborhood [26].

Local frequency estimation: The gray level intensities along ridges and valleys create a local neighborhood where no minutiae or singular points appear. This can be modeled as a sine-shaped

wave along the normal direction to the local ridge orientation. Former indicates that the local ridge frequency is another intrinsic property of a fingerprint image [26].

Region mask estimation: A fingerprint image has pixels or blocks that could be in a recoverable or unrecoverable region. This classification process can be done by evaluating the wave shape created by local ridges and valleys in terms of their amplitude, frequency, and variance [26].

Gabor filtering: An interesting characteristic of fingerprints is their inherent configuration of parallel ridges and valleys, which have a well-defined frequency and orientation providing useful information that helps eliminate unwanted noise. These characteristics help to eliminate undesired noise while preserving true ridges and valleys. Since the sinusoidal-shape waves from ridge-valley structures vary slowly in a local orientation, a well-tuned bandpass filter at a specific frequency and orientation can remove noise while preserving accurate ridge-valley structures. Gabor filters are suitable for bandpass filters because they have frequency-selective and orientation-selective properties, giving them optimal joint resolution in the spatial and frequency domains [28]. The even-symmetric Gabor filter has the general form:

$$h(x, y; \phi, f) = e^{-\frac{1}{2} \left[\frac{(x \cos \phi)^2}{\sigma_x^2} + \frac{(y \sin \phi)^2}{\sigma_y^2} \right]} \cos(2\pi f x \cos \phi), \quad (2)$$

where ϕ is the orientation of the Gabor filter, f is the frequency of the sinusoidal plane wave, and σ_x and σ_y are the space constants of the Gaussian envelope along the x and y axes, respectively. The application of Gabor filters to an image requires the following three parameters:

- The frequency of the sinusoidal plane wave
- The filter orientation
- The standard deviations of the Gaussian envelope

The first parameter corresponds to the local ridge frequency, and the second is the local ridge orientation. The third parameter involves a trade-off of values; the higher these values, the more resistant to noise the filters are, but this is more likely to create spurious ridges and valleys. In contrast, the smaller the values, the filters will not create spurious ridge-valley structures but will be less effective at removing noise. In this work, both values were implemented as 0.5. Using the estimated images, N as the normalized fingerprint, O as the orientation image, F as the frequency image, and R as the region mask, the enhanced image E is calculated as:

$$E(i, j) = \begin{cases} 255, & \text{if } R(i, j) = 0 \\ \sum_{u=-\frac{w_g}{2}}^{\frac{w_g}{2}} \sum_{v=-\frac{w_g}{2}}^{\frac{w_g}{2}} h(u, v; O(i, j), F(i, j)) N(i - u, j - v), & \text{otherwise} \end{cases} \quad (3)$$

where $w_g = 11$ is the size of the Gabor filters [26].

Binarization: The last step is implemented using a threshold in the enhanced image E using the following criteria:

$$B(i, j) = \begin{cases} 1, & \text{if } E(i, j) \geq 0 \\ 0, & \text{otherwise} \end{cases}, \quad (4)$$

where $B(i, j)$ is the binarized version of the fingerprint, concluding the preprocessing of the input images.

The following diagram presents the main steps in the enhancement algorithm used in this work:

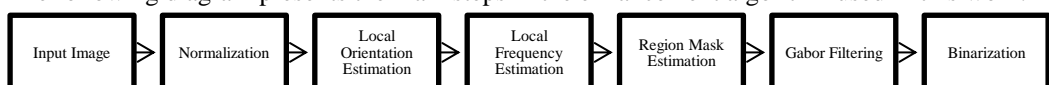


Figure 1. Flow diagram of the enhancement algorithm implemented.

An example of the enhancement algorithm is presented in Fig. 2 using a fingerprint from the FVC2000 database [23]. The initial image from the subset is illustrated in Fig.2.a. This image provides information regarding the ridge orientations shown in Fig.2.b. The red strokes indicate the angle (orientation) of the ridges. The next step involves the calculation of the ridge frequency used as an input for the Gabor filter presented in Fig.2.c. Lastly, binarization is performed to enhance the ridges and valleys from the initial fingerprint. The processed image will be composed with 0's on the ridges, and 1's on the valleys, as presented in Fig.2.d.

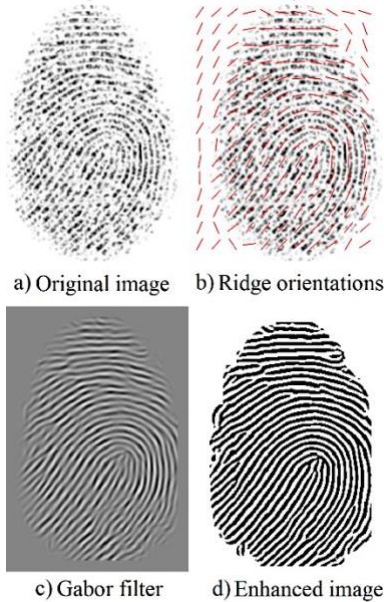


Figure 2. Preprocessing example of the input fingerprint images.

Step 2: Wavelet transform

A popular technique in image processing is the Wavelet transform. This approach was applied to extract information from the fingerprint images. More information about the Wavelet transform procedure is available in [9].

Step 3: Feature extraction using multiple domains

This stage describes multiple transforms calculated from each preprocessed fingerprint.

Gray Level Co-occurrence Matrix (GLCM): GLCM is a square matrix that provides specific properties about the spatial distribution of gray levels in the image's texture [29]. This matrix shows how often a reference pixel value with intensity i occurs in a specific relationship with another neighboring pixel with intensity j . In other words, each element (i, j) of the GLCM is the number of occurrences of the pixel pair at a distance d relative to each other [29]. This spatial relationship can be defined in multiple forms with different offsets and angles. For an image I of size $M \times N$, the elements of the corresponding GLCM for a displacement vector $d = (d_x, d_y)$ are defined as:

$$GLCM = \sum_{x=1}^M \sum_{y=1}^N \begin{cases} 1, & \text{if } I(x, y) = i \text{ and } I(x + d_x, y + d_y) = j, \\ 0, & \text{otherwise} \end{cases}, \quad (5)$$

In this work we consider one neighboring pixel $d = 1$ along with four possible directions $[0 \ 1]$ for 0° , $[-1 \ 1]$ for 45° , $[-1 \ 0]$ for 90° , and $[-1 \ -1]$ for 135° [17]. Each element of the GLCM is the number of times that two pixels with gray values i and j are neighbors in distance d and direction θ [29].

A regular histogram does not include the information about the relative position of the pixels; that is why for texture measurements, the GLCM is mainly used since it incorporates in the texture analysis not only the distribution of intensities but also the relative position of pixels in an image [30]. The number of possible intensity levels in the original image determines the size of the GLCM. We work with 8-bit images meaning there are 256 possible levels [30].

The GLCM is computed on the approximation image because the Wavelet transform decomposed the original image into these lower frequency coefficients ignoring the noise signals related to the higher frequencies, which are present in the detail coefficients [17]. Since this approximation has a lower resolution, it provides a compressed representation of the fingerprint image, allowing to ignore several extra details that are not relevant to the texture information for this specific application. The GLCM becomes a Wavelet co-occurrence matrix in the Wavelet domain. This matrix offers a second-order statistical texture representation of the input fingerprint image [17]. So far, we have only calculated the GLCM, but we need to compute the texture descriptors that will be a part of the feature set used for fingerprint recognition. To accomplish this objective, we applied the *graycoprops* function to generate four descriptors including contrast, correlation, energy, and homogeneity; whose equations are presented below:

$$Contrast = \sum_{i,j} |i - j|^2 GLCM_{i,j}, \quad (6)$$

$$Correlation = \sum_{i,j} \frac{(i - \mu_i)(j - \mu_j)GLCM_{i,j}}{\sigma_i \sigma_j}, \quad (7)$$

$$Energy = \sum_{i,j} GLCM_{i,j}^2, \quad (8)$$

$$Homogeneity = \sum_{i,j} \frac{GLCM_{i,j}}{1 + |i - j|}, \quad (9)$$

where the first-order statistics μ and σ are the mean and variance, respectively [17]. Since we use four different orientations, the total number of features per fingerprint is 16 as texture descriptors. For each orientation, the GLCM is calculated by applying its respective offset. That means that equations (6) – (9) must be used four times because the GLCM variable will have four different values, one for each offset.

Spatial domain, Fast Fourier Transform (FFT), and Discrete Cosine Transform (DCT): FFT and DCT coefficients were calculated using the normalized fingerprint image. Four features were computed from these coefficients, including the mean of standard deviations, the standard deviation of the means, the mean of the absolute deviations, and the standard deviation of the absolute deviations [18]. Similar features were also calculated from the spatial domain version, i.e., the normalized fingerprint image. Another feature was the pixel density from the binarized version of the fingerprint image.

Statistic measures from the Wavelet transform: A subsequent 2-D DWT was applied to the binarized fingerprints. In this step, we used the Wavelet base “db12”. Various statistic measures were calculated from each one of the detail coefficient images [21].

Wavelet-Bands Selection Features (WBSF): WBSF separates the horizontal and vertical coefficient details into sub-bands giving information in both directions. Based on the same 2-D DWT processed in the previous step, the mean and standard deviations of the sub-bands provide the set of 36 features from this step [19].

The total amount of features computed for each fingerprint image is 170. All the features are collected into a table and labeled with a categorical variable representing the fingerprint owner.

Step 4: Ensemble Subspace Discriminant Classifier

One of the benefits of ensemble classifiers is their capacity to merge results from various “weak” learners into a high-quality ensemble model. Linear Discriminant Analysis (LDA) classifiers were chosen as the individual learners used in this step. LDA is a fundamental data analysis method that establishes the lower dimension subspace in which the data points from the original problem are separable. This separability is specified in terms of mean and variance values [31]. The subspace discriminant algorithm has medium prediction speed and low memory usage. The main advantage of utilizing a subspace ensemble is less memory than ensembles with all predictors [32]. In [33] is presented a description of the steps executed by the random subspace algorithm.

5. Results and discussion. - The method proposed in this paper was implemented in MATLAB R2019b. The implementation included the application of several toolboxes, including the Wavelet toolbox, Image Processing toolbox, and Statistics and Machine Learning toolbox. More details regarding the specific functions used for signal processing are included in [9]. The Classification Learner application is an intuitive interface for training machine learning models. The feature table produced for each subset has a size of 80x171, 80 imprints of fingerprints (10 subjects with eight fingerprints per subject), and 171 features (including the categorical variable). The learners applied to create the ensemble are LDA classifiers. 10-fold cross-validation was employed to generalize the data and prevent overfitting. Table I summarizes the highest accuracy values obtained for the twelve subsets analyzed in this work.

Database	Accuracy
DB1-FVC2000	95 %
DB2-FVC2000	95 %
DB3-FVC2000	97.5 %
DB4-FVC2000	95 %
DB1-FVC2002	85 %
DB2-FVC2002	76.3 %
DB3-FVC2002	85 %
DB4-FVC2002	83.8 %
DB1-FVC2004	78.8 %
DB2-FVC2004	65 %
DB3-FVC2004	95 %
DB4_FVC2004	80 %

Table I. Results of the classification process for every database.

The preprocessing enhancement algorithm has shown high and acceptable performance for several subsets in the three databases included in this work. The following figure compares boxplots for the validation accuracies for all subsets used in this system.

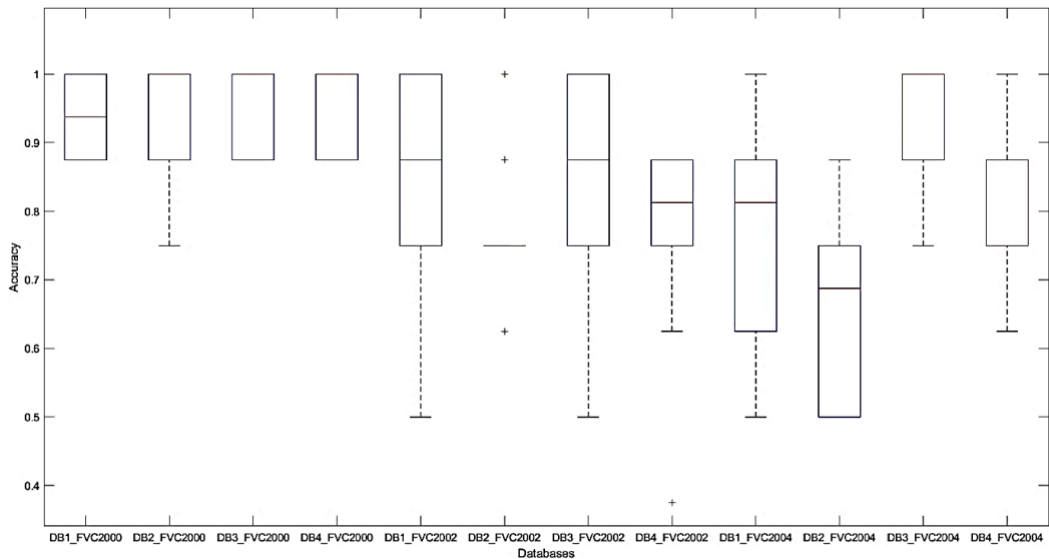


Figure 3. Boxplots of the accuracy values computed for each database.

The boxplots for the FVC2000 database (the first four boxplots) have a higher distribution for the quartiles, as can be noticed in Fig. 3. This behavior is consistent with the average accuracy values reported among the highest for all 12 subsets. On the contrary, the remaining eight subsets have wider quartiles, but almost for every classifier, the fingerprint verification system achieves a 100% accuracy for at least one-fold in the cross-validation implemented.

Another algorithm performance comparison is presented in the Receiver Operating Characteristic (ROC) curves. The positive class must be the same so a fair comparison can be made between all databases; in this case, Subject-Eight was chosen. Fig. 4 presents the results for the FVC2000 database.

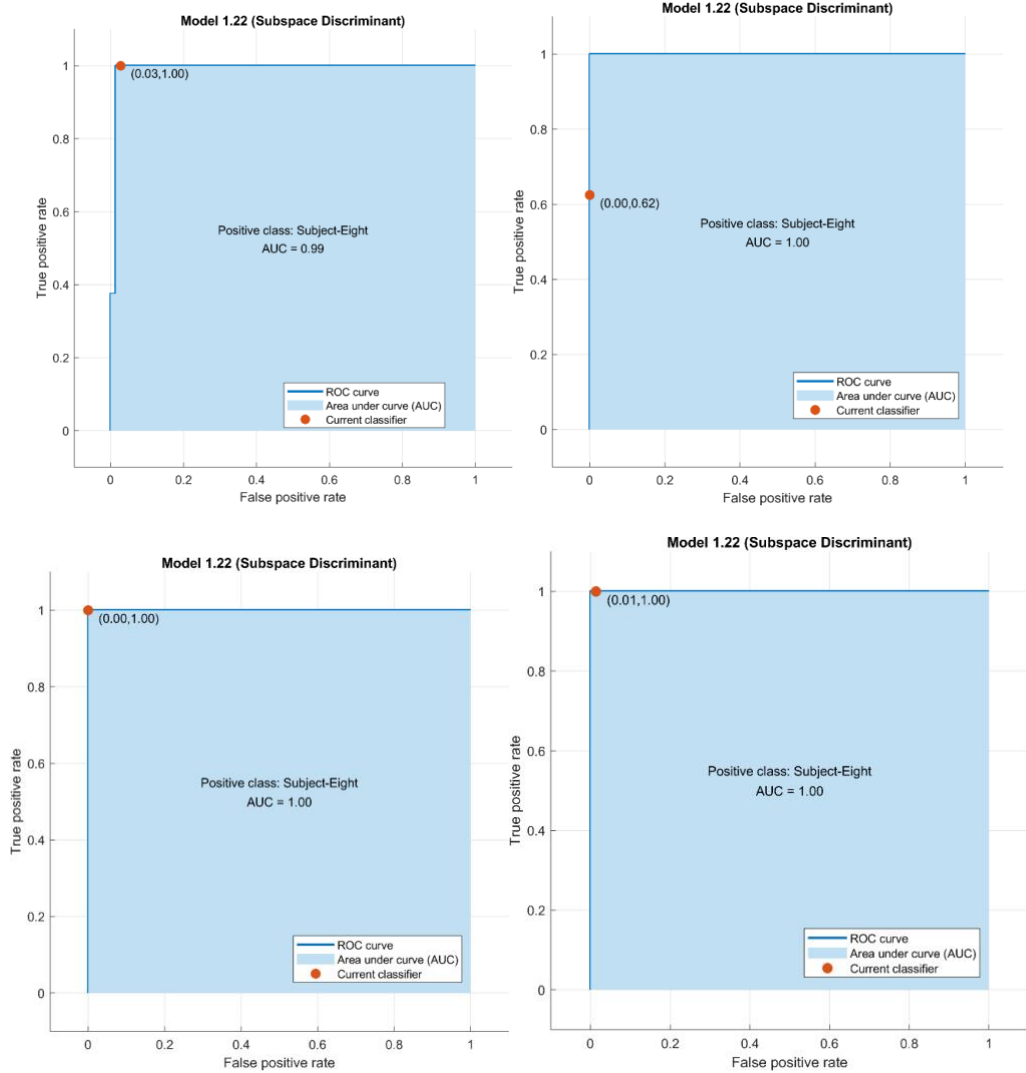


Figure 4. ROC curves for the FVC2000 database (Top left: DB1, top right: DB2, bottom left: DB3, bottom right: DB4).

A good classifier should have a ROC curve as close as possible to the top left, which in this case is true for the four subsets. As a result, we can prove again that high performance from the FVC2000 database can be inferred from the ROC curves presented. For the FVC2002 database, the next ROC curves were obtained.

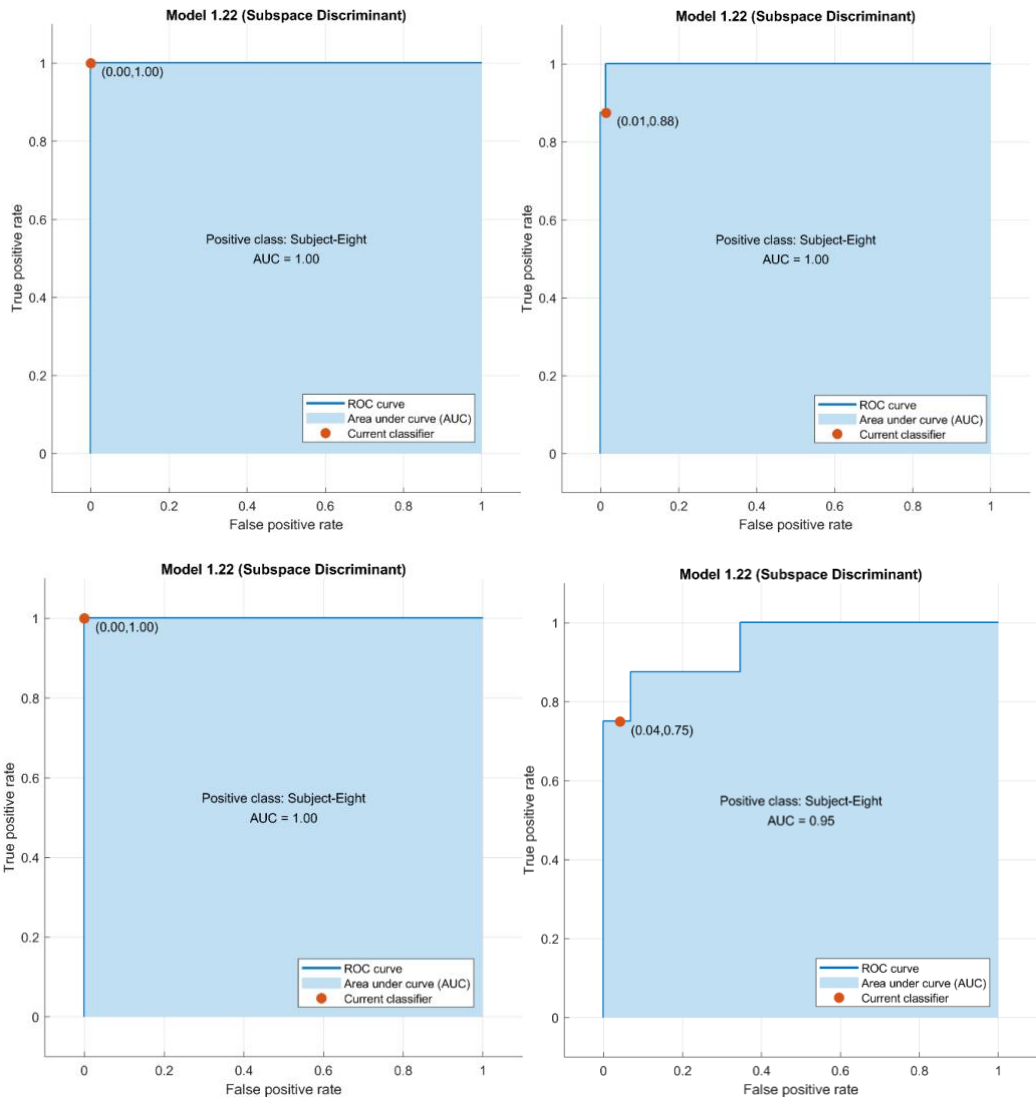


Figure 5. ROC curves for the FVC2002 database (Top left: DB1, top right: DB2, bottom left: DB3, bottom right: DB4).

For the FVC2002 database, it can be implied that for the DB4 subset, the algorithm performance is inferior, which is analogous to the lower accuracy value obtained for this subset at 83.8%. Finally, for the FVC2004, we have the following ROC curves.

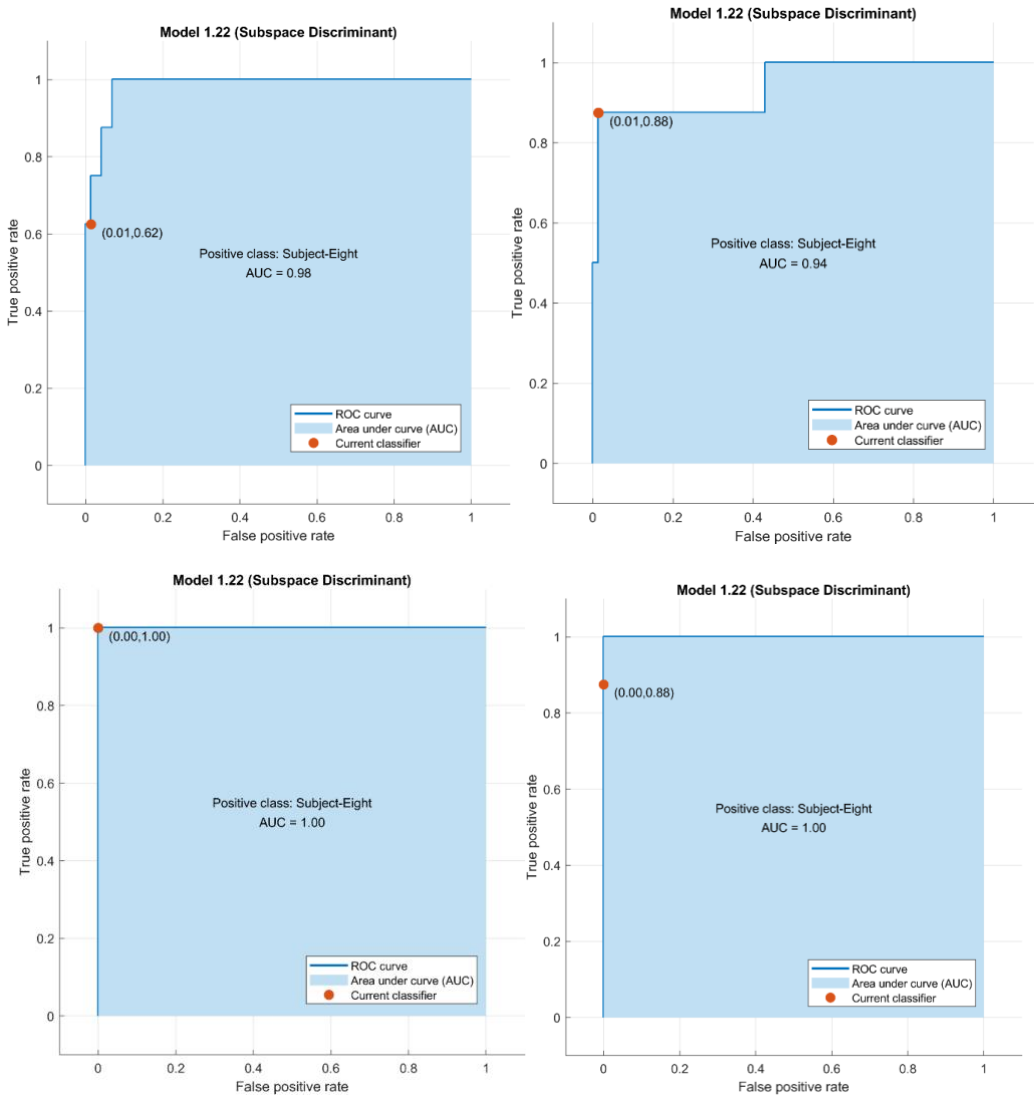


Figure 6. ROC curves for the FVC2004 database (Top left: DB1, top right: DB2, bottom left: DB3, bottom right: DB4).

This database provides the lowest accuracy values for the classification, which can be noticed from the ROC curves presented in Fig. 6. Note that these ROC curves were computed using only one positive class; if we choose a different class, we will obtain different results. The ROC curves will represent the behavior performance that was already reported using accuracy in Table I. To compare the performance of the classifiers from literature with the proposed method, we utilized the “accuracy” metric. This comparison is presented in Table II.

Work	Feature Extraction	Number of Features	Classification Model	Training Time	Database	Accuracy
Suwarno, et al. [5]	Haar-like transformation	100	Hamming distance	n/a	Custom set	80 %
Abdul-Haleem, et al. [6]	Energy, local ridge features, statistic measures, invariant moments	119	Absolute difference	n/a	DB3 (FVC2004)	96.87 %
Velapure, et al. [7]	Ridge contours, Gabor filter	≈ 16384	SVM	Not reported	Fingerprint Color Image.v1	87.5 %
Nguyen, et al. [10]	Statistic measures	256	Random forest	10 h 50 min	FVC group	95.8 %
Iloanusi, et al. [18]	Spatial, FFT, DCT, statistic measures	17	Manhattan distance	n/a	DB4 (FVC2000)	96.89 %
Tang, et al. [20]	Statistic measures, Shannon entropy	1152	Normalize Euclidean distance	n/a	FVC2000	96.84 %
Akbar, et al. [21]	DWT, PCA, DCT	40	SVM	Not reported	CASIA Version_5.0 (Dataset1)	95 %
Jirandeh, et al. [22]	Gabor Wavelet	160	SVM	≈ 170 s	PolyU HRF	95.5 %
This work	Spatial, FFT, DCT, GLCM, WBSF, statistic measures	170	Ensemble Subspace Discriminant	13.202 s	DB3 (FVC2000)	97.5 %

Table II. Comparison of results

The values in the table correspond to the highest accuracies achieved in each work. Our system obtained an accuracy of 97.5 % for the set “B” from the FVC2000 database subset DB3. A thorough description of Table II can be found in [9].

In this extended version, we have included a new column indicating each author’s database. Suwarno, et al. [5] used fingerprints captured by a commercial scanner, creating their own custom set, while Abdul-Haleem, et al. [6] used the DB3 subset from the FVC2004 database. Velapure, et al. [7] applied the Fingerprint Color Image Database.v1, from MATLAB Central File Exchange. Nguyen, et al. [10] used the FVC group database, but subsets were not specified. Iloanusi, et al. [18] applied the DB4 subset from the FVC2000 database, Tang, et al. [20] used the FVC2000 database. Akbar, et al. [21] utilized the CASIA Fingerprint Image Database Version_5.0 (Dataset1) and Jirandeh, et al. [22] used the PolyU HRF database. It is worth noting that although not all databases are the same, the comparison provides a good insight into the general performance of the proposed system in fingerprint verification research.

6. Conclusions. - This paper presents a fingerprint verification system based on DWT, multiple domain feature extraction, and Ensemble Subspace Classifier. The preprocessing algorithm used to enhance the original fingerprint images from the three datasets applies image processing techniques such as normalization, local orientation estimation, local frequency estimation, region estimation, and binarization. This work also explains why this approach is helpful for fingerprint image processing. This paper evaluated 12 fingerprint image subsets from which the highest accuracy (97.5 %, obtained for the DB3-FVC2000 subset) is compared with related works proposed in the literature.

7. References

- [1] S. Bharkad and M. Kokare, "Fingerprint identification — ideas, influences, and trends of new age," in *Pattern Recognition, Machine Intelligence and Biometrics*, Berlin, Springer, 2011, pp. 411-446.
- [2] P. Schuch, "Deep learning for fingerprint recognition systems," NTNU, 2019.
- [3] A. M. Bazen, *Fingerprint Identification: Feature Extraction, Matching, and Database Search*, Twente University Press, 2002.
- [4] National Research Council of the National Academies, "Biometric recognition: Challenges and opportunities," National Academies Press, Washington, 2010.
- [5] S. Suwarno and P. I. Santosa, "Simple verification of low-resolution fingerprint using non-minutiae feature," in *Journal of Physics: Conference Series*, 2019.
- [6] M. G. Abdul-Haleem, L. E. George and H. M. Al-Bayti, "Fingerprint recognition using haar wavelet transform and local ridge attributes only," *International Journal of Advanced Research in Computer Science and Software Engineering*, vol. 4, no. 1, pp. 122-130, 2014.
- [7] A. Velapure and R. Talware, "Performance analysis of fingerprint recognition using machine learning algorithms," in *Proc. of the Third International Conference on Computational Intelligence and Informatics*, 2020.
- [8] M. Leghari, S. Memon, F. Sahito, A. A. Chandio and M. Leghari, "Biometric verification enhancement with ensemble learning classifiers," in *2018 5th International Multi-Topic ICT Conference (IMTIC)*, 2018.
- [9] A. Rojas and D. G. Jovanovic, "Fingerprint recognition based on wavelet transform and ensemble subspace classifier," in *2021 IEEE URUCON*, Montevideo, 2021.
- [10] L. T. Nguyen, H. T. Nguyen, A. D. Afanasiev and T. V. Nguyen, "Automatic identification fingerprint based on machine learning method," *Journal of the Operations Research Society of China*, 2021.
- [11] M. A. Yaman, A. Subasi and F. Rattay, "Comparison of random subspace and voting ensemble machine learning methods for face recognition," *Symmetry*, vol. 10, no. 11, p. 651, 2018.
- [12] A. S. Ashour, Y. Guo, A. R. Hawas and G. Xu, "Ensemble of subspace discriminant classifiers for schistosomal liver fibrosis staging in mice microscopic images," *Health Information Science and Systems*, vol. 6, 2018.
- [13] K. Radhika and S. Varadarajan, "Ensemble subspace discriminant classification of satellite images," *Journal of Scientific and Industrial Research*, vol. 77, pp. 633-638, 2018.
- [14] S. Basheer, K. K. Nagwanshi, S. Bhatia, S. Dubey and G. R. Sinha, "FESD: An approach for biometric human footprint matching using fuzzy ensemble learning," *IEEE Access*, vol. 9, pp. 26641-26663, 2021.
- [15] M. I. Islam, N. Begum, M. Alam and M. R. Amin, "Fingerprint detection using canny filter and DWT, a new approach," *Journal of Information Processing Systems*, vol. 6, no. 4, pp. 511-520, 2010.
- [16] M. Tico, E. Immonen, P. Ramo, P. Kuosmanen and J. Saarinen, "Fingerprint recognition using wavelet features," in *ISCAS 2001. The 2001 IEEE International Symposium on Circuits and Systems*, 2001.

- [17] K. S. Jeyalakshmi and T. Kathirvalavakumar, "Haralick features from wavelet domain in recognizing fingerprints using neural network," in *International Conference on Mining Intelligence and Knowledge Exploration*, 2020.
- [18] O. Iloanusi, N. David, C. Osuagwu and S. Olisa, "Multiple domains and transform-based features for fingerprint matching," *International Journal of Scientific and Technology Research*, vol. 7, no. 9, pp. 27-34, 2018.
- [19] M. D. Al-Hassani, A. Kadhim and V. W. Samawi, "Fingerprint identification technique based on wavelet-bands selection features (WBSF)," *International Journal of Computer Engineering and Technology (IJCET)*, vol. 4, no. 3, pp. 308-323, 2013.
- [20] T. Tang, "Fingerprint recognition using wavelet domain features," in *2012 8th International Conference on Natural Computation (ICNC 2012)*, 2012.
- [21] S. Akbar, A. Ahmad and M. Hayat, "Identification of fingerprint using discrete wavelet transform in conjunction with support vector machine," *IJCSI International Journal of Computer Science Issues*, vol. 11, no. 5, pp. 189-199, 2014.
- [22] H. M. Jirandeh, H. Sadeghi and M. A. Javadi Rad, "High-resolution automated fingerprint recognition system (AFRS) based on gabor wavelet and SVM," *International Journal of Scientific and Engineering Research*, vol. 5, no. 5, pp. 166-169, 2014.
- [23] BioLab - University of Bologna, "FVC2000," 2000. [Online]. Available: <http://bias.csr.unibo.it/fvc2000/>. [Accessed 4 July 2022].
- [24] BioLab - University of Bologna, "FVC2002 - Second International Fingerprint Verification Competition," 2002. [Online]. Available: <http://bias.csr.unibo.it/fvc2002/>. [Accessed 4 July 2022].
- [25] Biometric System Lab - University of Bologna, "FVC2004 - Third International Fingerprint Verification Competition," 2003. [Online]. Available: <http://bias.csr.unibo.it/fvc2004/>. [Accessed 4 July 2022].
- [26] L. Hong, Y. Wan and A. Jain, "Fingerprint image enhancement: Algorithm and performance evaluation," *IEEE Transactions on Pattern Analysis and Machine Intelligence*, vol. 20, no. 8, pp. 777-789, 1998.
- [27] P. Kovesi, "MATLAB and Octave Functions for Computer Vision and Image Processing," 2000. [Online]. Available: <https://www.peterkovesi.com/matlabfns/#fingerprints>. [Accessed 17 February 2021].
- [28] A. K. Jain and F. Farrokhnia, "Unsupervised texture segmentation using gabor filters," *Pattern Recognition*, vol. 24, no. 12, pp. 1167-1186, 1991.
- [29] B. Pathak and D. Barooah, "Texture analysis based on the gray-level co-occurrence matrix considering possible orientations," *International Journal of Advanced Research in Electrical, Electronics and Instrumentation Engineering*, vol. 2, no. 9, pp. 4206-4212, 2013.
- [30] R. C. Gonzalez, R. E. Woods and S. L. Eddins, *Digital Image Processing Using MATLAB*, Gatesmark Publishing, 2009.
- [31] P. Xanthopoulos, P. Pardalos and T. Trafalis, "Linear discriminant analysis," in *Robust Data Mining*, Springer, 2013, pp. 27-33.
- [32] T. K. Ho, "The random subspace method for constructing decision forests," *IEEE Transactions on Pattern Analysis and Machine Intelligence*, vol. 20, no. 8, pp. 832-844, 1998.

[33] MathWorks, "Ensemble Algorithms," The MathWorks, Inc., [Online]. Available: https://www.mathworks.com/help/stats/ensemble-algorithms.html#mw_58afb400-8bf3-448f-aaf2-2a2e749a3faa. [Accessed 6 April 2021].

Nota contribución de los autores:

1. Concepción y diseño del estudio
2. Adquisición de datos
3. Análisis de datos
4. Discusión de los resultados
5. Redacción del manuscrito
6. Aprobación de la versión final del manuscrito

AR ha contribuido en: 1, 2, 3, 4, 5 y 6.

GJD ha contribuido en: 1, 2, 3, 4, 5 y 6.

Nota de aceptación: Este artículo fue aprobado por los editores de la revista Dr. Rafael Sotelo y Mag. Ing. Fernando A. Hernández Gobertti.